Effect of molecular weight of tyramine-modified hyaluronan on polarization state of peripheral blood mononuclear cells-derived macrophages

Jacek K. Wychowaniec,*[a] Ezgi Irem Bektas,[a] Andrea J. Vernengo,[a] Marcia Mürner,[a,b] Marielle Airoldi,[a] David Eglin[c] and Matteo D'Este[a]

[a] AO Research Institute, Clavadelerstrasse 8, Davos, 7270, Switzerland

[b] ETH Zürich, Zürich, 8093, Switzerland

[c] Mines Saint-Étienne, Univ Jean Monnet, INSERM, U1059 Sainbiose, Saint-Étienne, France

*Corresponding author J.K.W.
Phone: (+41)0779238956; e-mail: jacek.wychowaniec@aofoundation.org

Graphical Abstract

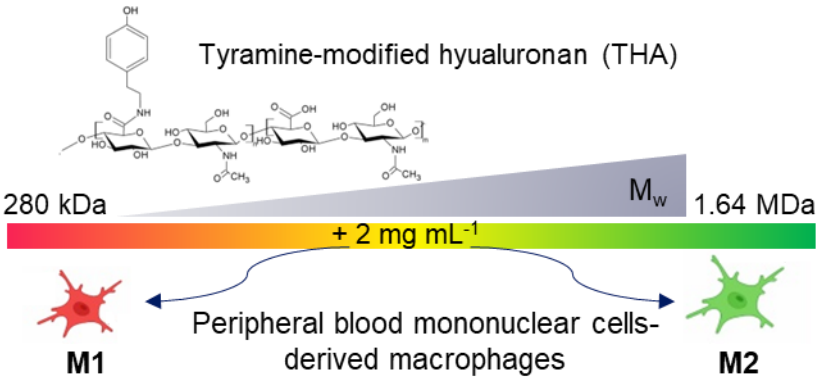

Abstract

The immunomodulatory properties of hyaluronan and its derivatives are key to their use in medicine and tissue engineering. In this work we evaluated the capability of soluble tyramine-modified hyaluronan (THA) of two molecular weights (low M_w=280 kDa and high M_w=1640 kDa) for polarization of peripheral blood mononuclear cells-derived macrophages. We demonstrate the polarization effects of the supplemented THA by the semi-automated image analysis from confocal microscopy, immunofluorescent staining utilising CD68 and CD206 surface markers, RT-qPCR gene expression analysis, as well as using the enzyme-linked immunosorbent assay (ELISA). The expression of certain cytokines including TNF-α (pro-inflammatory), IL-10 (anti-inflammatory) and surface marker CD206 are more viable options for rapid screening of polarization states of macrophages with CD206 marker being associated with the lowest donor variability. Our findings indicate that low M_w THA can be associated with mild pro-inflammatory state, M1-like state, whereas high M_w THA can be associated with mild pro-regenerative, M2-like state, and that the extent of these responses are donor-dependent. The variation in the obtained phenotypic responses may stem from possible uncontrolled genetic factors in received blood donor samples. Finally, we confirm the typical association of low versus high molecular weight for THA holds true and stipulate that these responses will provide more accurate *in vivo* representation and translational

immunomodulatory guidance for the use of THA-based biomaterials to a wider biomaterials and tissue engineering communities.

Keywords: Tyramine-modified hyaluronan; Peripheral blood mononuclear cells-derived macrophages; Macrophage Polarization; Inflammation; Immunomodulation

1. Introduction

Generating and manipulating a complexity of custom instructive cellular signals during regenerative processes is key to engineer biopolymers for biomedical applications. It is well established that the immune system is vital in inducing normal healing of damaged tissues, mediated by both innate and adaptive immunity, mainly by inflammation [1-5]. During injury, the immune system can have both beneficial and detrimental effects that improve tissue repair or escalate degeneration, in a context-dependent manner [6-9]. These opposing effects are associated with the phenotypic state of the immune cells present at the injury site. The complexity of cell types and signalling pathways involved in inflammatory and/or degenerative processes encompasses a vast array of immune cells, including T cells, B cells, dendritic cells, monocytes, neutrophils and macrophages, as well as cytokines, chemokines, growth factors, and molecular interactions between all components, creating a highly intricate and multifaceted network that orchestrates the progression and resolution of any pathological process [10, 11]. Macrophages are often considered among the most important immune cells due to their versatile and central role in the immune system, particularly by their key role in producing a wide range of cytokines and chemokines that drive subsequent clearance and tissue resolution [12]. In the last decade new macrophage sub-types were discovered as part of innate immunity and have been shown to play crucial regulatory role in successful tissue regeneration [13]. Macrophages thus exist in a spectrum of polarization that ranges from a pro-inflammatory and detrimental ‘M1-like’ state to a protective anti-inflammatory ‘M2-like’ state [7, 9, 14-16]. M1-like and M2-like macrophages are two distinct phenotypes of macrophages with contrasting characteristics and functions. M1-like macrophages are activated in response to pathogens, such as interferon-gamma (IFN-γ) and lipopolysaccharides (LPS) from bacteria), produce high levels of pro-inflammatory cytokines (IL-1β, IL-6, and TNF-α) and nitric oxide, efficiently present antigens to T helper 1 (Th1) cells, and overall promote inflammation and host defence.

On the other hand, M2-like macrophages are activated in response to anti-inflammatory signals (including IL-4, IL-13, IL-10, and glucocorticoids), are involved in tissue remodelling, producing arginase-1, and promoting wound healing and immunosuppression [13, 17]. Overall surface markers including CD163, CD206, and CD209 are characteristic of M2-like activation [13, 18]. In general, the relative abundance of these macrophage phenotypes can shift dynamically during the course of tissue damage and repair, with M1-like state mostly present in early inflammatory phase of an acute injury and M2-like appearing through resolution and repair phase. Hence, time-dependent immunomodulation towards a certain state offers the opportunity to enhance functional and histopathological recovery [19, 20]. Although this traditional description of polarization spectrum remains a relatively simplistic classification of a true dynamic system of macrophages [17], in this work we retain adoption of the terms 'M1-like' and 'M2-like' to define general pro-inflammatory and anti-inflammatory states, respectively. Typical immune signalling pathways convert external stimuli into cytosolic events that lead to the resolution of infection, associated with downstream adaptors and effectors undergoing substantial conformational changes and spatial reorganization upon ligand engagement [21, 22]. Importantly, this process can be also achieved by: i) the use of appropriate materials providing biochemical and physical cues, or ii) by therapeutic administration of immunomodulatory molecules [23]. The final macrophage fate is driven by the complex interplay between external environmental signals and hardwired differentiation programming capabilities. In light of this, many recent studies have shown that certain biomaterials have inherent immunomodulatory properties capable of reducing the damaging innate inflammatory response caused by macrophage infiltration, both *in vitro* and *in vivo* [24-26]. For example, engineered matrices enriched in immunomodulatory factors were shown to induce enhanced bone formation by promoting greater vascular invasion and instructed earlier inflammation [25].

Hyaluronan (HA) is a linear, anionic polysaccharide known to play a major biological role in a plethora of human tissues [27], and used as an effective biomaterial in tissue engineering [28-31]. Depending on its modal molecular weight (M_w) and extrinsic environment, HA has been shown to influence multiple biological pathways, including influencing paracrine signalling of neighbouring immune cells [32, 33]. This occurs through HA interactions with RHAMM (receptor for HA mediated motility) and CD44 principal receptors [34]. Particularly, CD44 receptor can distinguish M_w of HA and subsequently deliver contradictory signals to active different biological processes [35]. For example Rayahin *et al.* demonstrated on murine macrophages (J774A.1) that high molecular weight (>1000 kDa) HA can polarize macrophages to an M2-like phenotype, whereas low molecular weight HA (<1000 kDa) drives pro-inflammatory M1-like polarization [36]. More recently Lee *et al.* have concurred with original work demonstrating that high molecular-weight HA (>1250 kDa) inhibited pro-inflammatory responses in lipopolysaccharides (LPS)-stimulated RAW 264.7 murine macrophages and in concentration-dependent way induced anti-inflammatory responses [37]. Whilst many effects hold true for the mice or rat-derived macrophages, typically polarization state are more variable in human-derived cells due to known donor variability [38-40]. The effects of HA M_w have also been shown to be directly linked to the underlying endotoxin levels, potentially diminishing in the full absence of endotoxins [38, 39, 41]. In one case, the high molecular weight HA (M_w=1010–1800 kDa) triggered an effective polarization of primary human monocytes (THP-1 cells) towards an M2-like state [42]. To date variable results were noted, with an overall polarization of macrophages to HA depending on the exact cell type and source, concentration, M_w and associated endotoxin levels. These however have not been provided for chemically functionalized versions of HA, which are more commonly used across tissue engineering and regenerative medicine fields.

Recently, tyramine-modified hyaluronan (THA) has been shown to be one of the effective biopolymers and building blocks of therapeutic biomaterials enabling rapid biofabrication and cellular attachment by means of both enzymatic (horseradish peroxidase, H_2O_2) and light-based crosslinking (e.g. Eosin and green light irradiation) methods [43-47]. THA has also been used in conjugation with collagen as an extrudable bioink capable of topographical induction of cellular alignment and migration [48]. Recently part of our group investigated the effect of THA (M_w=280 kDa) hydrogels along various other biomaterials, on neutrophils, indicating relative immuno-inertness and lack of enhanced pro-inflammatory response compared to other studied materials [24].

We stipulate that designing functional biomaterials that incorporate immunomodulatory effects, biocompatibility and that allow stable long-term polarization of macrophages is therefore of high interest in tissue engineering and biofabrication [23], and hence in the current work we evaluated the capability of macrophage polarization of THA of two molecular weights: M_w=280 kDa (LMW THA) and M_w=1640 kDa (HMW THA), supplemented in cell culture medium at lower concentration, as a soluble signal. Such signal is expected to: (i) occur as a released factor from three-dimensional THA-based crosslinked biomaterials as fragmented parts of uncrosslinked polymeric networks/detached sites from THA-based biomaterials, or (ii) be used as simple carbohydrate supplementation to medium. The polarization effects of the supplemented THA on macrophages differentiated from human peripheral blood mononuclear cells (PMBCs) were evaluated on cells from three donors. M1-like and M2-like polarization modulated by the supplementation with THA were unravelled by the immunofluorescent staining, gene expression analysis and ELISA.

2. Materials and methods

2.1. Synthesis and characterisation of tyramine-modified hyaluronan (THA)

THA of two molecular weights: M_w=280 kDa (abbreviated throughout as LMW THA) and M_w=1640 kDa (abbreviated throughout as HMW THA) were synthesized as previously described [45, 49]. Briefly, sodium hyaluronate (Contipro Biotechs.r.o., Czech Republic) was dissolved in deionized H_2O at 1 w/v%. THA conjugates were prepared in a one-step reaction by addition of 1.25 mmol 4-(4,6-dimethoxy-1,3,5-triazin-2-yl)-4-methylmorpholinium chloride (DMTMM, TCI Europe N.V.) coupling agent and subsequently 1.25 mmol tyramine hydrochloride (Roth, 5234.3) was added dropwise to the solution. The reaction was carried out at 37 °C and under continuous stirring for 24 h. The product was purified via precipitation with 96% ethanol after the addition of 10 v/v% saturated sodium chloride. Several wash steps were performed, and the product kept under vacuum for 72 h, with first 24 hours at 25°C and then for two final days at 40°C. For HMW THA, the purification and washing were repeated twice to ensure complete removal of trapped H_2O and ethanol. Proton nuclear magnetic resonance spectroscopy (^{1}H NMR, 300 MHz, Bruker Avance III) and UV absorbance measurements at 275 nm on Infinite® 200 Pro plate reader (Tecan, Männedorf, Switzerland) were performed to confirm the degree of substitution (DoS) of tyramine on HA (with $DoS_{LMW\ THA}$= 6.01 ± 0.57 %, and $DoS_{HMW\ THA}$= 5.99 ± 0.57 %). ^{1}H NMR data is presented in ***Figure S1***. Loss of drying (LOD) was also evaluated. For that, 100 mg of THA was weighted into a glass vial and dried under vacuum at 105°C for 24 h. LOD was then calculated following the formula:

$$\text{LOD (\%)} = \frac{W_b - W_a}{W_b} \text{ x } 100\% \qquad (1)$$

, where W_b defines weight of THA before drying and W_a defines weight of THA after drying. The following values were obtained: $LOD_{LMW\ THA}$= 9.8 ± 0.5 %, and $LOD_{HMW\ THA}$= 12.8 ± 0.5 %.

2.2. Endotoxin analysis

Bacterial endotoxins (lipopolysaccharides, LPS)-cell wall material from gram negative bacteria is a commonly known molecule that can activate immune cells [50]. To evaluate the

LPS content of THA, the endotoxin content was measured using the Pierce™ Chromogenic Endotoxin Quant Kit (Thermo-Fisher) according to the manufacturer's instructions. To evaluate THA, we adapted our previous protocol [24], and prepared enzymatically crosslinked THA hydrogels at 3.5 w/v% with 0.1 U mL^{-1} Horseradish peroxidase (HRP) 0.15 mM H_2O_2, the same for both LMW and HMW THA. The THA hydrogels were directly prepared in the wells and were incubated for 1 hour with endotoxin free H_2O (Sigma-Aldrich). An endotoxin standard stock solution was prepared by adding endotoxin free H_2O (Sigma-Aldrich) to the E. coli endotoxin standard vial to create a high standard (0.1-1.0 EU mL^{-1}) and a low standard (0.01-0.1 EU mL^{-1}). After 1 hour the supernatant H_2O was harvested from the THA hydrogels and transferred to the pre-warmed readout plate at 37 °C as well as two standard curves were prepared on this plate. The amoebocyte lysate reagent was added to each well and the plates were incubated for 8 min at 37 °C. The reaction of the chromogenic substrate solution was stopped after 6 min at 37 °C by adding 25 v/v% acetic acid to each well and the optical density was measured at 405 nm using the Infinite® 200 Pro plate reader (Tecan, Männedorf, Switzerland). The obtained values were used to calculate the concentration based on the provided standard curve for the aforementioned concentration ranges, with R^2=0.98 and R^2=0.95 for low and high standards, respectively.

2.3. Peripheral blood mononuclear cells (PBMCs)-derived macrophages cell culture

Primary human monocytes were isolated from buffy coats purchased from the Regional Blood Donation Service SRK Graubünden (Chur, Switzerland) from three human donors (D1, D2 and D3) using Ficoll density gradient separation. No donor information was received as per local regulations. Obtained peripheral blood mononuclear cells (PMBCs) were labelled with CD14 magnetic beads followed by magnetic-activated cell sorting (MACS) [51, 52]. $CD14^+$ monocytes cells were resuspended in RPMI medium supplemented with 10% FBS and then seeded onto tissue culture plastic at a density of 1.82 x 10^5 cells $well^{-1}$ for D1, and at a density

of 3.0 x 10^5 cells $well^{-1}$ for donors D2 and D3, both in the presence of 20 ng mL^{-1} human macrophage colony-stimulating factor (hM-CSF) for 5 days. Medium (still containing hM-CSF) was exchanged on day 2. At day 5, hM-CSF-free medium was supplemented with 10 ng mL^{-1} TNF-α and IFN-γ for M1-like macrophages and 10 ng mL^{-1} IL-4 for M2-like macrophages for 24 hours followed by a 24-hour rest in medium without cytokines (***Figure 1***). Positive control samples (M0-like macrophages) were cultured in medium without any cytokines (***Figure 1***). Furthermore, on day 5, the same three polarization states were maintained (M0, M1, M2), either without any external influence of materials, or in the presence of the 2 mg mL^{-1} LMW THA and HMW THA supplemented in the cell culture medium (***Figure 1***). Noteworthy, 2 mg mL^{-1} of both LMW and HMW THA remained liquid and did not result in a formation of any self-supporting physical hydrogels. On day 7, conditioned medium was collected, samples were washed two times with PBS and fixed with 4% formaldehyde for 20 minutes for immunofluorescent staining and stored in TRI-reagent for subsequent RNA isolation (***Figure 1***).

2.4. Immunofluorescence analysis

D1 samples for immunofluorescent analysis were stained for nucleus with DAPI (NucBlue® Fixed Cell ReadyProbes® Reagent, ThermoFisher), and for phalloidin (ActinGreen™ 488 ReadyProbes® Reagent, ThermoFisher). Samples were firstly permeabilized with 0.25% Triton X-100 in PBS for 30 minutes and subsequently washed two times with wash buffer (0.05% Tween-20 in PBS). Samples were then firstly stained with phalloidin and left for 1 hour in darkness. Subsequently, they were washed again two times with wash buffer, and finally incubated with DAPI for 10 mins in darkness. Manufacturers' instructions were followed for DAPI and ActinGreen dilutions (1 drop per 0.5 mL).

D3 samples for immunofluorescent analysis were stained for nucleus with DAPI (NucBlue® Fixed Cell ReadyProbes® Reagent, ThermoFisher), for phalloidin (ActinRed™ 555

ReadyProbes® Reagent, ThermoFisher), for MMR/CD206 (M2-like macrophage surface marker) with Alexa Fluor® 700 (FAB25342N, R&DSystems, Bio-Techne), and for CD68/SR-D1 (a glycoprotein marker that is primarily found on the surface of macrophages) with Alexa Fluor® 488 (IC20401G, R&DSystems, Bio-Techne). Samples were firstly permeabilized with 0.25% Triton X-100 in PBS for 30 minutes and subsequently washed once with wash buffer. Samples were then firstly stained with phalloidin and left for 3 hours in darkness. Subsequently, they were washed one time with wash buffer, and then incubated with blocking solution (1% BSA in 1x PBS) for 1 hour. Then samples were washed one time with wash buffer and incubated with CD68 or CD206 staining (separate wells) pre-made at 8 µg mL^{-1} with 0.1% BSA in PBS overnight in darkness. Subsequently samples were washed one more time with wash buffer and incubated with DAPI for 10 mins. Manufacturers' instructions were followed for DAPI and ActinRed dilutions (1 drop per 0.5 mL). D2 samples were used to establish the appropriate staining protocol, subsequently used, and described above for D3 samples.

Samples were analysed using confocal microscope (Zeiss LSM800 Airyscan Confocal Microscope) with channels at 405 nm (DAPI), 561 nm (ActinRed), 515 nm (ActinGreen/CD68 Alexa Fluor 488) and 723 nm (CD206, Alexa Fluor 700).

Image analysis (nucleus cell area and circularity, cytoskeleton's area as well as CD68 area) was performed using ImageJ® on images taken using 10x objective. Only areas in the range from 5 to 120 μm^2 and 90 to 400 μm^2 were taken into consideration, for nucleus and cytoskeleton, respectively. For CD68 analysis, 10 to 400 μm^2 areas were taken into consideration. Smaller areas would be indicative of fragments whereas larger were excluded based on threshold found in manual analysis indicating more than 2 nuclei/cytoskeleton of cells overlapping with each other/touching.

2.5. RNA isolation and RT-qPCR gene analysis

To assess the polarization of macrophages, cells were collected and seeded in a 24-well plate at a concentration and with treatments described in section 2.3. RNA was isolated with salt precipitation and TaqManTM Reverse Transcription Kit was used to generate cDNA. Relative gene expression reactions were set up in 10 µL reaction mixes using TaqManTM MasterMix, relevant human primers (***Table 1***), diethyl pyrocarbonate treated water (DEPC-water) and cDNA. Real-time polymerase chain reaction (real-time PCR) was performed on two technical duplicates for n=4 (D1) or n=3 (D2 and D3) repeats, using QuantStudio 7 Flex. The relative gene expression was identified using $2^{-\Delta\Delta Ct}$ value with RPLP0 as endogenous control and positive control (M0-like macrophages, no supplemented material) were used for normalization.

Table 1. Human primer sequences for real-time PCR

MARKER	ASSAY ID (THERMOFISHER)	ROLE
TNF-α	Hs00174128_m1	Pro-inflammatory marker (associated with M1-like macrophages)
IL-6	Hs00174131_m1	
IL-1β	Hs00174097_m1	
INOS	Hs01075529_m1	
IL-10	Hs00961622_m1	Anti-inflammatory marker (associated with M2-like macrophages)
CD206	Hs00267207_m1	M2-like macrophage surface marker
RPLP0		Forward: *5'-TGG GCA AGA ACA CCA TGA TG-3'* Reverse: *5'-CGG ATA TGA GGC AGC AGT TTC-3'* Probe: *5'-AGG GCA CCT GGA AAA CAA CCC AGC-3'* Housekeeping gene

2.6. Enzyme-linked immunosorbent assay (ELISA)

At the end of each polarization experiment, supernatant media was collected and kept for measurements of pro-inflammatory (IL-1β, IL-6, TNF-α) and anti-inflammatory (CD163, IL-10) cytokines, describing M1-like and M2-like macrophages, respectively. . The DuoSet ELISA systems were used according to the manufacturer's instructions (DY201, DY206, DY210, DY1607, DY217B, R&D Systems, respectively). Absorbance values were measured

on Infinite® 200 Pro plate reader (Tecan, Männedorf, Switzerland) at 450 nm with a background wavelength correction of 540 nm.

2.7. Statistical analysis

All results were analysed and presented with GraphPad Prism version 9.3.1. Results are shown as an average ± standard deviation (SD), with individual points marked. To perform statistical significance one-way analysis of variance (ANOVA) with Šídák's multiple comparisons was used. A statistically significant results were considered as of $p<0.05$ (ns - >0.05, * - <0.05, ** - <0.01, *** - <0.005 and **** - <0.001).

3. Results and discussion

3.1. Endotoxins analysis

To eliminate the possible effects stemming from the endotoxins, we confirmed that their measured levels were 0.27 ± 0.07 U mL^{-1} and 0.26 ± 0.04 U mL^{-1} for LMW THA and HMW THA, respectively, below the limit for clinical medical devices of 0.5 EU mL^{-1} set by the Food and Drug Administration (FDA) [53]. Given that endotoxin levels were similar for both LMW and HMW THA, we anticipate that any unravelled differences due to THA in polarisation experiments discussed throughout this article will stem solely from the difference in M_w.

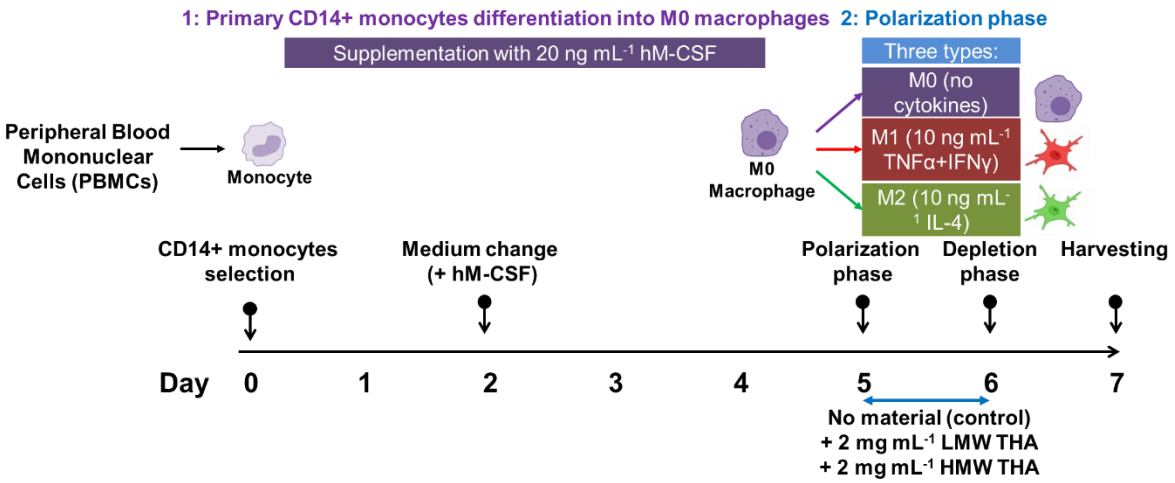

Figure 1. Differentiation protocol and subsequent characterisation of peripheral blood mononuclear cells (PBMCs)-derived macrophages. *PBMCs were differentiated into M0 macrophages over 5 days period by supplementation with 20 ng mL^{-1} human macrophage colony-stimulating factor (hM-CSF). At day 5, differentiated M0 macrophages were polarized*

by medium supplemented with 10 ng mL^{-1} TNF-α and IFN-γ towards an M1-like state and 10 ng mL^{-1} IL-4 towards an M2-like state for 24 hours, followed by a 24-hour rest in medium without cytokines. Positive control samples (M0-like macrophages) were cultured in medium without any cytokines. The same three polarization states were maintained (M0, M1, M2), either without any external influence of materials (control), or in the presence of the 2 mg mL^{-1} LMW THA and HMW THA supplemented in the cell culture medium at day 5.

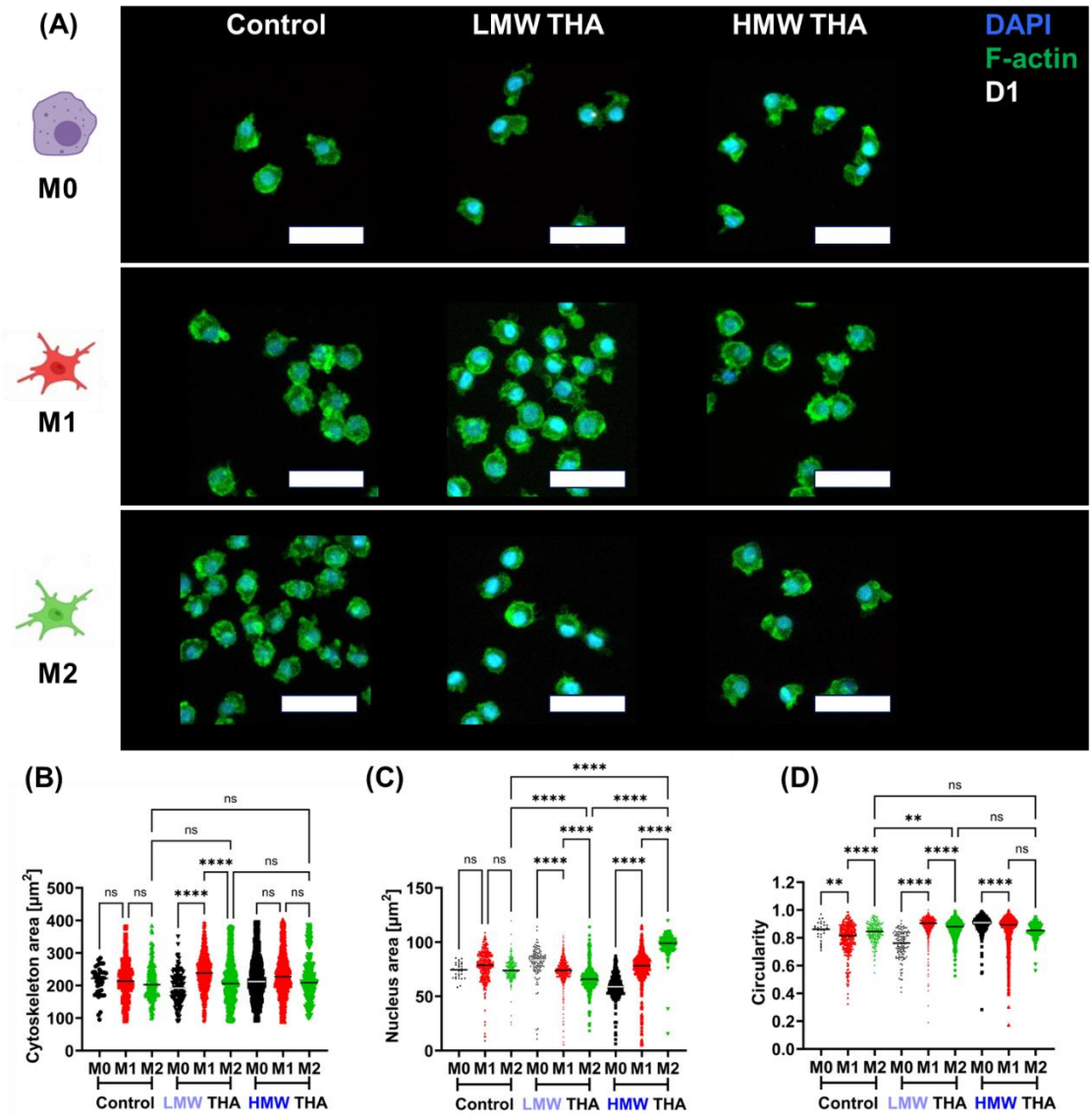

Figure 2. Immunofluorescence characterisation of D1 peripheral blood mononuclear cells (PBMCs)-derived macrophages. (A) *Immunofluorescence staining of nucleus by DAPI (**blue**) and F-actin by Phalloidin (**green**) for all tested groups in D1. Images were digitally enlarged to higher magnification to enable visualization of individual cells. Original images with lower magnification are provided in supporting information **Figure S3**. Each raw represents different polarization state (M0, M1 and M2) and columns represent a control and samples supplemented with 2mg mL^{-1} LMW or HMW THA. Scale bar = 50 µm. ImageJ analysis of obtained for at least 100 cells for all groups of: **(B)** cytoskeleton area, **(C)** nucleus area and **(D)** nucleus circularity. Analysis by one-way ANOVA with Šídák's multiple comparisons test. A statistically significant results were considered for p<0.05 (* - <0.05, ** - <0.01, *** - <0.005 and **** - <0.001).*

3.2. Cellular architecture parameters analysis

We first aimed to confirm the polarisation protocol of peripheral blood mononuclear cells (PBMCs)-derived macrophages (***Figure 1***) indeed influences the cellular response, hence at day 6, after the cytokine's depletion, we evaluated using bright field microscopy the preliminary changes in cellular shape as a function of all polarization states and supplemented materials (***Figure S2***). Indeed, qualitatively more elongated cells were obtained across both M1 and M2 states, indicative of cellular changes. Moreover, more cellular protrusions (i.e. filopodia) were observed across all M1 groups, in line with previous observations for M1-like type of macrophages [54, 55]. To confirm these findings, we firstly stained F-actin filaments and DAPI and performed immunofluorescence assay (on D1, from samples harvested from day 7 of polarization protocol) with semi-quantitative image analysis (***Figure 2***). Fluorescent images confirmed similar findings that macrophages polarised *in vitro* to an M1 phenotype exhibited distinctly more lamellar processes, were of more elongated shape, whereas an M2 phenotype resulted in cells that were partly similar in shape to unpolarised M0 macrophages, with fewer lamellar processes. Furthermore, evidently macrophages cultured in the presence of LMW THA appeared to have more filopodia and processes stemming from cellular bodies compared to control and HMW THA groups (***Figure 2A***). This trend has been confirmed with the significant differences in cellular areas between M0 and M1, and M1 and M2 groups ($p<0.001$, ***Figure 2B***), indicating an influence of LMW THA on the polarization state of macrophages. The highest cellular area was observed for M1 phenotype, concurring with some previous observations [56]. For comparison, there were no significant differences noted for cells in either control or HMW THA groups across all polarization states (***Figure 2B***). For control group, there were also no statistical differences in the area of nucleus between all polarization states (***Figure 2C***). However clear influence of LMW and HMW were observed, with nuclei area

decreasing from M0 to M1 to M2 ($p<0.001$) in LMW THA group, and the nuclei area increasing from M0 to M1 to M2 in the presence of HMW THA (***Figure 2C***). Other reports suggest possible decrease of nuclear area for M1 phenotypes [55], although no statistical significance was provided. In our case, the effects of modulation of nuclear area by M_w of THA in macrophage phenotypes are apparent, with opposing trends obtained for LMW and HMW THA groups. In the control group, the circularity of M1 macrophages was lowest (***Figure 2D***, $p<0.01$), which concurred with previous observations of human primary macrophages on fibrous architectures [57]. On the other hand, this trend of circularity was modulated by the presence of LMW THA, with M0 group having lower circularity, similar to that of M1 in control group, indicating potential pro-inflammatory influence of LMW THA (***Figure 2D***). However, M1 group in LMW THA retained higher circularity, therefore indicating an opposite trend, with the effects stemming from LMW THA and supplemented 10 ng mL^{-1} TNF-α and IFN-γ of polarization cytokines, mitigating each other. Although this analysis provides useful insights into modulatory potential of M_w of THA, its effects may be limited and, in this case, D1-specific.

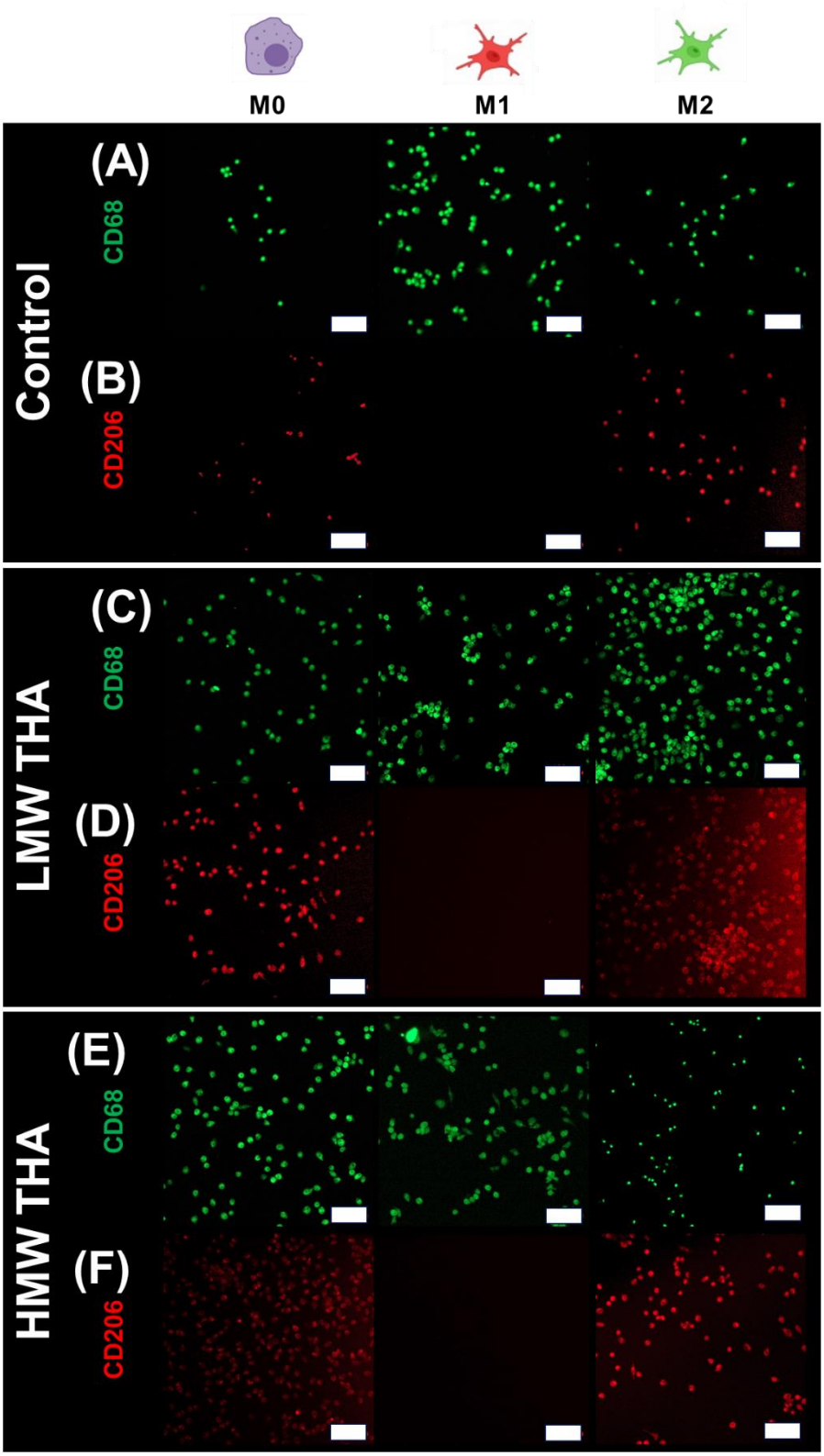

Figure 3. Immunofluorescent characterisation of D3 peripheral blood mononuclear cells (PBMCs)-derived macrophages. *Staining of CD68 (**green**) is shown in panels **(A)**, **(C)**, and **(E)**; whereas staining of CD206 (**red**) is shown in panels **(B)**, **(D)**, and **(F)**. Each column represents different polarization state (M0, M1 and M2) as indicated on the top. **(A)** and **(B)** represent panels for a control, **(C)** and **(D)** represent samples supplemented with 2mg mL^{-1} LMW THA, and **(E)** and **(F)** represent samples supplemented with 2mg mL^{-1} HMW THA. Scale*

*bar for all images = 100 µm. All images containing full images including staining of nucleus by DAPI (**blue**) and F-actin by Phalloidin (**orange**) are presented in **Figure S4**.*

3.3. M1 and M2 surface receptors analysis.

To further investigate the propensity for M1 versus M2 polarisation, we performed immunofluorescent staining using CD68, often associated as typical M1-like marker [18, 58], and CD206 as M2-like marker (***Figure 3***) [59, 60]. CD68 is typically located in the endosomal/lysosomal compartment however it has been shown to rapidly shuttle to the cell surface, particularly for M1-like macrophage phenotype [18, 58]. In the control group, CD68 expression has been present in all polarization states mainly in endosomal compartment (M0, M1, M2, ***Figure 3A***), with its expression extending outside to the cell surface predominately for M1-like phenotype, indicative of the pro-inflammatory polarization state. This is further supported by the largest CD68 staining area for M1 state across a control group (***Figure S5***). In contrary, expression of CD206 was most evident in M2 polarization state in control group, with only some evidence of cells expressing it in M0 state (***Figure 3B***). M1 state did not show any expression of CD206, as expected for the three polarization states. LMW THA was associated with stimulated expression of CD68 for all three polarization states (***Figure 3C***, ***Figure S5***), with some evidence of more spreaded cells for M1, similar to the expected trend in cytoskeletal area spreading (***Figure 2B***). In all polarization groups, CD68 extended from endosomal compartment, with highest CD68 area in M2 state (***Figure S5***). The area of CD68 and its overall expression appeared upregulated in the presence of LMW THA (***Figure S5***). On the other hand, LMW THA induced higher expression of CD206 in M0 group, indicating its potential pro-regenerative polarization in cells (***Figure 3D***). As expected, no CD206 signal was observed in M1 state. In M2 group, the CD206 staining appears, however partly diffused throughout sample, confirming that LMW THA does not significantly suppress this expression in the presence of supplemented 10 ng mL^{-1} IL-4 (***Figure 3D***).

In M0 and M1 states, HMW THA we observed the CD68 expression extending from endosomal compartments, whereas in M2 case, clearly more endosomal expression of CD68 was present (***Figure 3E***, ***Figure S5***). On the other hand, HMW THA M0 group showed significantly higher area of CD68 staining than LMW THA M2 group ($p<0.001$), indicating predominance of HMW THA for expression of CD68 (***Figure S5***). However, this effect was significantly supressed by synergetic action with supplemented 10 ng mL^{-1} IL-4, in which case clear retention of CD68 in endosomal compartment was evident, with lowest area across all tested groups (***Figure S5***), indicating a more synergetic pro-regenerative action. This was further confirmed in CD206 staining, where there was relatively weak expression for M0 state, no expression in M1 state and strong expression in M2 state (***Figure 3F***), in the presence of HMW THA. The immunocytochemistry results point to the pro-regenerative role of supplemented HMW THA and somewhat more complex role of LMW THA compared to the control groups. Quantification of phenotypic states using immunofluorescent CD206 is also relatively hard as the exact fluorescence signal depends on the staining protocol, laser power, sample incubation time, location, age of sample (length of time kept before imaging occurs), among others and hence here was only used qualitatively. To unravel more complex dependence on donors, we next run RT-qPCR gene analysis of most common markers, including CD206 expression.

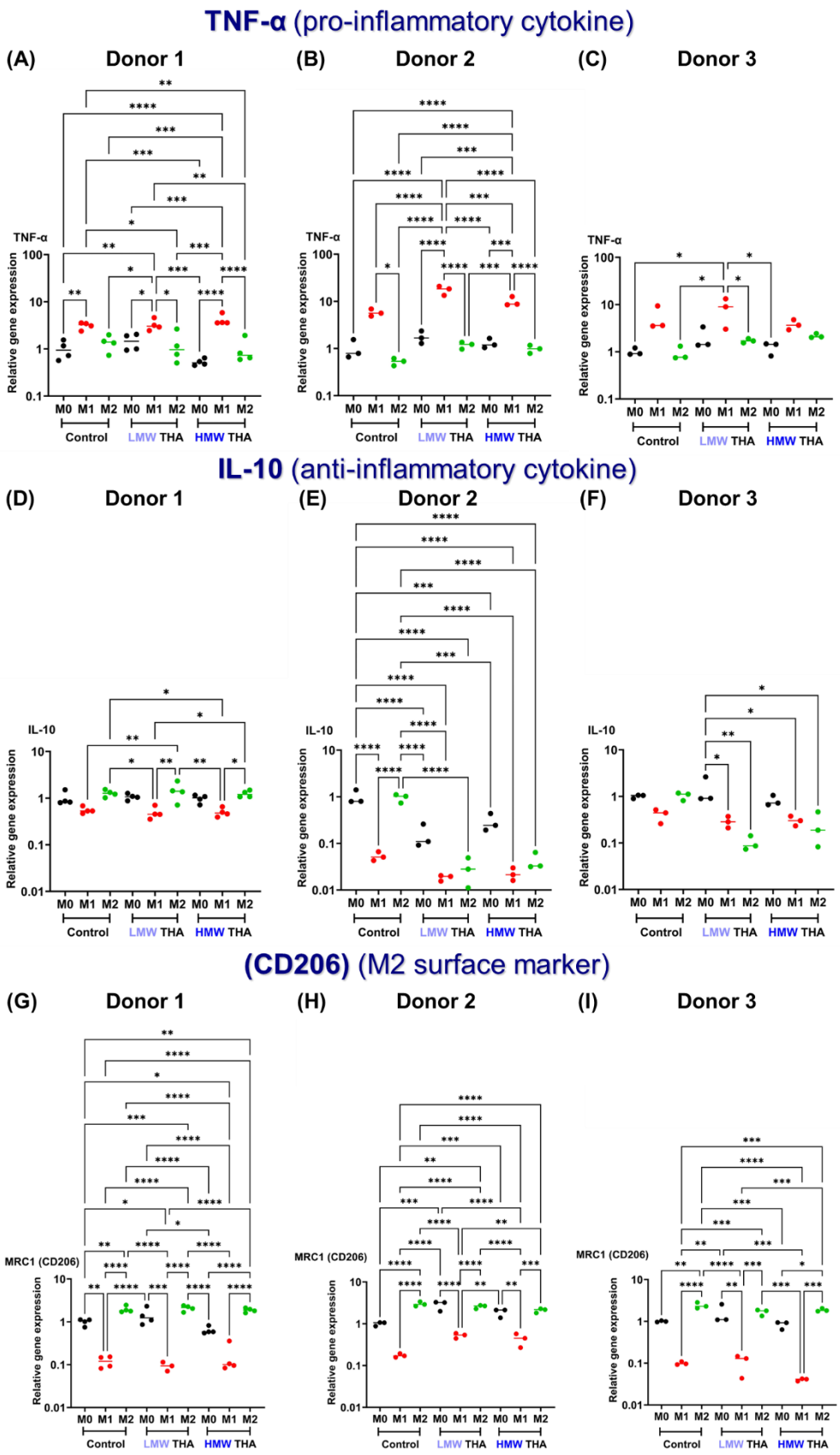

Figure 4. *Gene expression of* ***(A-C)*** *TNF-α,* ***(D-F)*** *IL-10,* ***(G-I)*** *MRC1 (CD206), measured by RT-qPCR for cells without any material conditioning (control) or encapsulated with 2mg mL^{-1} LMW or HMW THA. Data is represented for three cases: i) M0 without any*

*additional stimulation, ii) M1 pre-stimulated by the addition of 10 ng mL^{-1} TNF-α and IFN-γ and iii) M2 pre-stimulated by the addition of 10 ng mL^{-1} IL-4. For each gene, each panel presents data from individual donor, with **(A)**, **(D)**, **(G)** for D1, **(B)**, **(E)**, **(H)** for D2 and **(C)**, **(F)**, **(I)** for D3. For easier identification, each polarization state has been marked by distinct colour on all graphs in the following way: ● - M0 ● - M1 ● - M2. Gene expression is represented as fold change compared to RPLP0 (a housekeeping gene) of the M0 control group. Data represent n=4 for D1 and n=3 for D2 and D3 of individual experiments. Analysis by one-way ANOVA with Šídák's multiple comparisons test. A statistically significant results were considered for p<0.05 (* - <0.05, ** - <0.01, *** - <0.005 and **** - <0.001).*

3.4. Gene expression analyses – intra versus inter-donor variability.

First, we evaluated a panel of markers (***Table 1***) consisting of pro-inflammatory markers (TNF-α, IL-6, IL-1β, iNOS), an anti-inflammatory marker (IL-10) and M2 surface marker (CD206), on D1 samples (***Figure S6*** and ***Figure 4A, D, G***). Out of all pro-inflammatory markers, only TNF-α indicated significant differences between polarization groups and groups containing LMW and HMW THA (***Figure 4A***), with no significant differences observed for the remaining pro-inflammatory markers (***Figure S6***). On the other hand, we detected significant differences between both anti-inflammatory IL10 marker and CD206 surface markers associated with an M2 state in D1 samples (***Figure 4C, G***). Hence, to fully evaluate intra-donor variability we run full gene expression analysis on TNF-α, IL10 and CD206, with the upregulated TNF-α predominantly representing M1-like state and upregulated IL10 and CD206 representing an M2-like state [61]. We believe that for the purpose of this work the adopted association of M1-like and M2-like states is sufficient and adequately informative to provide influence of the supplemented factors and THA of variable M_w.

As expected, for all donors, we observed significant upregulation in TNF-α, evident in each M1 group as compared to M0, of both D1 and D2 (***Figure 4A-B***), however not statistically significant in D3 (***Figure 4C***). The exception to this was LMW THA M1 group as compared to M0 control (***Figure 4C***), potentially demonstrating the mild synergetic effect in D3 of LMW THA and pro-inflammatory cytokine polarization effects. Another evidence of potential role of LMW THA is comparison of LMW THA M1 group versus M1 control group in D2,

$p<0.001$, (***Figure 4B***), indicating higher upregulation expression of TNF-α in the presence of LMW THA. The same higher upregulation is statistically significant between LMW THA and HMW THA M1 groups in D2, $p<0.005$ (***Figure 4B***). This effect was not as evident in D1 and D3, hence pointing to the fact that modulation of LMW THA is, as expected, donor dependent. In fact, if all data is pulled together to evaluate inter-donor comparisons, no significant differences were observed at all (***Figure S7A***) in the upregulation of TNF-α. Finally, in all cases, M2 state in all groups had similar expression to M0 state, both with and without the presence of THA (lack of significance, ***Figure 4A-C***), demonstrating lack of induced pro-inflammatory state for all M2 groups. We note that variations in regulation of TNF-α across donors may come from both environmental and genetic factors, including gender, white blood cells, tobacco consumption, and cholesterol levels [62]. These factors are not provided or controlled in the received blood donations.

In the case of IL-10, an anti-inflammatory marker, we observed significant differences between all donors (***Figure 4D-F***). In D1, we observed upregulation of IL-10 in THA M2 groups, with $p<0.05$ for HMW and $p<0.01$ for LMW THA (***Figure 4D***), indicating, as expected, pro-regenerative state of M2-like states. IL-10 was severely downregulated in all M1 groups in D2 (***Figure 4E***), indicating, as expected, suppression of pro-regenerative state. However, somewhat unexpected, the same downregulation was observed in M2 groups in LMW and HMW THA groups (D2), but not in the control group, potentially indicating that THA of both M_w influenced the typical JAK/STAT IL-10 production metabolic pathways in macrophages, and that certain donors may have propensity for this pathway's dysregulation [63]. Similar disruption was observed in LMW THA group in D3 with both M1 and M2 groups downregulating IL-10 (***Figure 4F***). As expected, due to this donor variability, the pulled data showed no significant differences between any groups (***Figure S7B***). The interpretation of the overall IL-10 gene regulation data is intricate as human IL-10 regulation has been shown to be

affected by interindividual variation in gene expression [64, 65]. We therefore believe that responses that we see in our data stem directly from the variation introduced by host genetic factors, which are not pre-screened in received blood donations.

In the case of CD206 surface marker, its upregulation was evident and coherent across all donors, with all M2 groups upregulated compared to M1 in control, LMW and HMW THA groups (***Figure 4G-I***). Furthermore, M2 was also upregulated compared to M0 for D1 in control and HMW THA groups (***Figure 4G***), for D2 in control group (***Figure 4H***) and for D3 in control and HMW THA groups (***Figure 4I***). Interesting, the most evident donor variation was observed in the case of D2, for whom LMW THA M0 group was upregulated ($p<0.005$) as compared to M0 control group, indicating that LMW THA contributed to the larger abundance of mannose receptor 1 (CD206) on macrophage surface. This corroborated well with previously shown immunofluorescence staining (***Figure 3D***). Although CD206 is typically associated with M2-like state of macrophage, it has been shown that its activation is associated with response to the overall inflammatory state [66], which is the case of LMW THA for D2. Hence, minor differences between donors were observed, however overall, more consistent CD206 regulation response was evident across all donors. In fact, this was the only marker with clear evidence of M2 upregulation and M1 downregulation when all donor data was combined (***Figure S7C***), making CD206 a predominant surface marker for evaluation of the overall macrophage polarization state.

From the gene expression experiments, the major outcomes point to the fact that LMW THA has higher tendency to influence the polarisation state of the macrophages as compared to control and HMW THA groups, in a donor-dependent manner. The supplementation of LMW THA appears to have induced a mild inflammatory state in our model, whereas supplementation of HMW THA resulted in largely unchanged inflammation profile from typical control groups. The gene expression results are confirmatory to the observed

fluorescence staining imaging for D3 (***Figure 3*** and ***Figure 4***). To further investigate this trend, in the last step we evaluated cytokine expression by performing ELISAs on selected cytokines and donors.

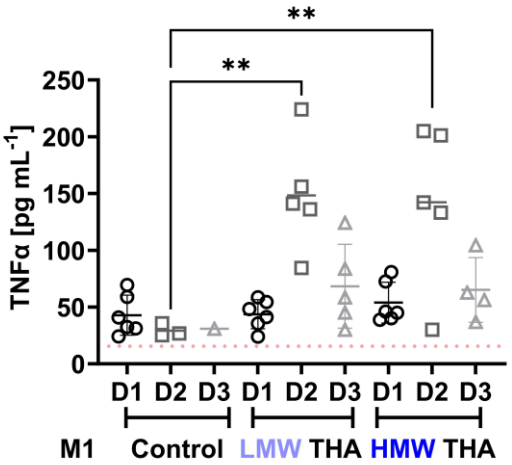

Figure 5. *TNF-α secretion measured by ELISA for cells without any material conditioning (control) or encapsulated with 2 mg mL^{-1} LMW or HMW THA, represented for each donor (D1, D2 and D3). Data is represented only for the M1 state, pre-stimulated by the addition of 10 ng mL^{-1} TNF-α and IFN-γ. The secretion for the other two cases (M0 and M2) in any other group was below the limit of detection, represented by the dotted line. Analysis by one-way ANOVA with Šídák's multiple comparisons test. A statistically significant results were considered for p<0.05 (* - <0.05, ** - <0.01, *** - <0.005 and **** - <0.001).*

3.5. Cytokine expression confirmation.

Secretion of TNF-α was below the limit of detection (LoD) of 15.6 pg mL^{-1} for all M0 and M2 states across all groups (control, LMW and HMW THA), and was only evident in M1 groups of all donors (***Figure 5***), confirming most pro-inflammatory profile already discussed. For D1 and D3, there were no significant differences between control, LMW or HMW conditions, whereas for D2, secretion of TNF-α was higher in the case of both LMW and HMW THA, ($p<0.01$, ***Figure 5***). This indicated predominant pro-inflammatory action of supplemented THA and susceptibility of D2 to it, and reaffirmed TNF-α gene expression (***Figure 4B***).

We have also evaluated secretion of IL-6, IL-10, IL-1β, and CD163 for D1, and IL-10 and CD163 for D2 and D3. For none of the donors we detected any IL-10 (with the LoD of 31.3 pg mL^{-1}), corroborating with the gene expression data showing no significant upregulation for any of the groups and polarization states. IL-1β for D1 has also not been detected for any of the groups (with LoD = 3.91 pg mL^{-1}). In D1, IL-6 was largely undetected (LoD=9.38 pg mL^{-1}) for control and HMW groups (***Figure S8A***), and only low amounts were detected in LMW THA group (in all states, M0, M1 and M2), pointing out to the potential pro-inflammatory action of supplemented LMW THA. Given that no IL-6 was detected for any HMW THA states, this further supports the idea that LMW THA tends to shift overall state towards mild pro-inflammatory state in this model. The soluble surface marker CD163 has been shown to play a crucial role in the resolution of inflammation [67]. On one hand site, it is has been often associated with tumour macrophages and more M2-like state [68], however more recently studies indicate that its presence is not always one-sided and these cells are highly plastic, with both M1 and M2 macrophages being able to express it [69]. This rather spectral view of CD163 was confirmed in our case, as we have detected none for D2 (LoD=156 pg mL^{-1}), and variable amounts for D1 (***Figure S8B***) and D3 (***Figure S8C***). The only statistically significant difference was observed between M1 state of control group and M0 state of LMW THA for D1, again indicative of more inflammatory-like state in the presence of LMW THA (***Figure S8B***). On the other hand, no significant differences were observed between any polarisation states or groups in D3 (***Figure S8B***). This indicates that CD163, although often describing well the polarisation states, is strongly donor dependent.

4. Conclusions

In summary here we unravel polarization tendencies of peripheral blood mononuclear cells (PBMCs)-derived macrophages upon supplementation with soluble chemically

tyramine-modified hyaluronan (THA) biopolymer signals, which constitute an important building block for many biomaterials or their released fragments. We demonstrate that different M_w of THA display different tendencies, with molecular weight of 280 kDa (defined here as LMW THA), showing a lenient trend for pro-inflammatory state, towards an M1-like modulation, in a donor dependent manner, as unravelled by the immunocytochemistry, gene expression analysis and ELISAs. THA with M_w=1640 kDa (referred to here as HMW THA) has been associated with mild pro-regenerative capacity polarizing macrophages towards an M2-like state, in a donor dependent manner. We acknowledge limitations associated with the current research, stemming from possible uncontrolled genetic factors in received blood donor samples. Here we also show that in our case, the expression of certain cytokines including TNF-α (pro-inflammatory), IL-10 (anti-inflammatory) and surface marker MRC1 (CD206, pro-regenerative marker) are more viable options for rapid screening of polarization states of macrophages derived from PBMCs, as compared to other factors (IL-6, IL-1β, iNOS, or CD163), which either showed overall low expression/secretion (IL-6, IL-1β, iNOS) or a very high donor variability (CD163). This view may also be associated with a limited number of cells available from each donor for experiments, overall limiting potential for screening using large cell densities. Finally, using traditional simplistic approach of “M1-like” as pro-inflammatory, and “M2-like” to as anti-inflammatory states, respectively, we confirm the typical association of low versus high molecular weight for chemically tyramine-modified hyaluronan holds true and we thus bring immunomodulatory guidance towards the appropriate choice of it to a wider biomaterials and tissue engineering communities. We believe that these responses provide more rapid and accurate *in vivo* representation and will provide translational basis for the use of THA-based biomaterials in the future.

Author Contributions

J.K.W.: Conceptualization, data curation, formal analysis, funding acquisition, investigation, methodology, project administration, resources, supervision, validation, visualization, writing - original draft, writing – review & editing; **E.I.B.**: Data curation, investigation, methodology, writing – review & editing; **A.J.V.**: Data curation, investigation, methodology, writing – review & editing; **M.M.**: Data curation, investigation, methodology; **M.A.**: investigation, methodology; **D. E.**: Conceptualization, funding acquisition, supervision, writing – review & editing; **M.D.**: Conceptualization, funding acquisition, methodology, project administration, resources, supervision, writing – review & editing.

Funding sources

This work was supported by the European Union's Horizon 2020 (H2020-MSCA-IF-2019) research and innovation programme under the Marie Skłodowska-Curie grant agreement 893099 — ImmunoBioInks and by the Leading House for the Middle East and North Africa for Research Partnership Grant 2022 "Space ImmunoBioInks" (RPG-2022-38). J.K.W. and M.D'E. also acknowledge the European Union's Horizon 2020 research and innovation programme under the grant agreement No 857287 (BBCE) as well as funding provided by AO Foundation.

Acknowledgements

The authors thank Nicolas Devantay for his technical support, particularly with the THA synthesis.

Supplementary data

Supplementary data available: ^{1}H NMR spectra of synthesized THA; bright field microscopy images; additional imageJ analysis and immunofluorescence images, RT-qPCR gene analysis an ELISA results. Supplementary data to this article can be found online at XYZ.

Conflicts of interest

There are no conflicts to declare.

Notes

All research data supporting this publication are directly available within this publication and associated supporting information.

ORCID numbers of authors:

Jacek K. Wychowaniec: https://orcid.org/0000-0002-6597-5242

Ezgi Irem Bektas: https://orcid.org/0000-0002-3700-5708

Andrea J. Vernengo: https://orcid.org/0000-0002-5143-7435

Marcia Mürner: https://orcid.org/0009-0006-5305-2113

David Eglin: https://orcid.org/0000-0002-8500-6887

Matteo D'Este: https://orcid.org/0000-0002-0424-8172

References

[1] K. Minton, Nature Reviews Immunology, 17 (2017) 277.
[2] C.H. Bucher, C. Schlundt, D. Wulsten, F.A. Sass, S. Wendler, A. Ellinghaus, T. Thiele, R. Seemann, B.M. Willie, H.-D. Volk, G.N. Duda, K. Schmidt-Bleek, Frontiers in Immunology, 10 (2019) 797.
[3] B. Zhang, Y. Su, J. Zhou, Y. Zheng, D. Zhu, Advanced Science, 8 (2021) 2100446.
[4] B. Shan, X. Wang, Y. Wu, C. Xu, Z. Xia, J. Dai, M. Shao, F. Zhao, S. He, L. Yang, M. Zhang, F. Nan, J. Li, J. Liu, J. Liu, W. Jia, Y. Qiu, B. Song, J.-D.J. Han, L. Rui, S.-Z. Duan, Y. Liu, Nature Immunology, 18 (2017) 519.
[5] S.R. Paludan, T. Pradeu, S.L. Masters, T.H. Mogensen, Nature Reviews Immunology, 21 (2021) 137-150.

[6] R. Rust, J. Kaiser, The Journal of neuroscience : the official journal of the Society for Neuroscience, 37 (2017) 4658-4660.
[7] J.C. Gensel, B. Zhang, Brain Research, 1619 (2015) 1-11.
[8] S. David, A. Kroner, Nat Rev Neurosci, 12 (2011) 388-399.
[9] K.A. Kigerl, J.C. Gensel, D.P. Ankeny, J.K. Alexander, D.J. Donnelly, P.G. Popovich, The Journal of Neuroscience, 29 (2009) 13435.
[10] P. Fang, X. Li, J. Dai, L. Cole, J.A. Camacho, Y. Zhang, Y. Ji, J. Wang, X.-F. Yang, H. Wang, Journal of Hematology & Oncology, 11 (2018) 97.
[11] L. Chen, H. Deng, H. Cui, J. Fang, Z. Zuo, J. Deng, Y. Li, X. Wang, L. Zhao, Oncotarget, 9 (2017).
[12] G. Arango Duque, A. Descoteaux, Frontiers in Immunology, 5 (2014).
[13] T. Lawrence, G. Natoli, Nature Reviews Immunology, 11 (2011) 750-761.
[14] S. Gordon, 3 (2003) 23-35.
[15] S. Kobashi, T. Terashima, M. Katagi, Y. Nakae, J. Okano, Y. Suzuki, M. Urushitani, H. Kojima, Mol Ther, 28 (2020) 254-265.
[16] S.F. Ma, Y.J. Chen, J.X. Zhang, L. Shen, R. Wang, J.S. Zhou, J.G. Hu, H.Z. Lü, Brain Behav Immun, 45 (2015) 157-170.
[17] Peter J. Murray, Judith E. Allen, Subhra K. Biswas, Edward A. Fisher, Derek W. Gilroy, S. Goerdt, S. Gordon, John A. Hamilton, Lionel B. Ivashkiv, T. Lawrence, M. Locati, A. Mantovani, Fernando O. Martinez, J.-L. Mege, David M. Mosser, G. Natoli, Jeroen P. Saeij, Joachim L. Schultze, Kari A. Shirey, A. Sica, J. Suttles, I. Udalova, Jo A. van Ginderachter, Stefanie N. Vogel, Thomas A. Wynn, Immunity, 41 (2014) 14-20.
[18] M.H.M. Barros, F. Hauck, J.H. Dreyer, B. Kempkes, G. Niedobitek, PLOS ONE, 8 (2013) e80908.
[19] C.M. Walsh, J.K. Wychowaniec, L. Costello, D.F. Brougham, D. Dooley, Advanced Healthcare Materials, (2023) 2300951.
[20] P. Wang, Y. Zhang, H. Lei, J. Yu, Q. Zhou, X. Shi, Y. Zhu, D. Zhang, P. Zhang, K. Wang, K. Dong, J. Xing, Y. Dong, Carbohydrate Polymers, 316 (2023) 121018.
[21] Q. Xiao, C.K. McAtee, X. Su, Nature Reviews Immunology, 22 (2022) 188-199.
[22] J. Lu, J. Qian, Z. Xu, S. Yin, L. Zhou, S. Zheng, W. Zhang, Frontiers in Cell and Developmental Biology, 9 (2021).
[23] C.M. Walsh, J.K. Wychowaniec, D.F. Brougham, D. Dooley, Pharmacology & Therapeutics, 234 (2022) 108043.
[24] M.A. Wesdorp, A. Schwab, E.I. Bektas, R. Narcisi, D. Eglin, M.J. Stoddart, G.J.V.M. Van Osch, M. D'Este, Bioactive Materials, 20 (2023) 627-637.
[25] A. García-García, S. Pigeot, I. Martin, Bioactive Materials, 24 (2023) 174-184.
[26] J. Sapudom, M. Kongsema, A. Methachittipan, S. Damrongsakkul, S. Kanokpanont, J.C.M. Teo, M. Khongkow, K. Tonsomboon, P. Thongnuek, Journal of Materials Chemistry B, 11 (2023) 3607-3616.
[27] B.P. Toole, Nature Reviews Cancer, 4 (2004) 528-539.
[28] K. Salma-Ancane, A. Sceglovs, E. Tracuma, J.K. Wychowaniec, K. Aunina, A. Ramata-Stunda, V. Nikolajeva, D. Loca, International Journal of Biological Macromolecules, 208 (2022) 995-1008.
[29] M. Halperin-Sternfeld, A. Pokhojaev, M. Ghosh, D. Rachmiel, R. Kannan, I. Grinberg, M. Asher, M. Aviv, P.X. Ma, I. Binderman, R. Sarig, L. Adler-Abramovich, Journal of Clinical Periodontology, 50 (2023) 200-219.
[30] W. Guo, L. Douma, M.H. Hu, D. Eglin, M. Alini, A. Šećerović, S. Grad, X. Peng, X. Zou, M. D'Este, M. Peroglio, Carbohydrate Polymers, 277 (2022) 118828.
[31] Q. Wei, Z. Jin, W. Zhang, Y. Zhao, Y. Wang, Y. Wei, X. He, G. Ma, Y. Guo, Y. Jiang, Z. Hu, Carbohydrate Polymers, 303 (2023) 120469.

[32] K.L. Aya, R. Stern, Wound Repair and Regeneration, 22 (2014) 579-593.
[33] D.-M. Kuang, Y. Wu, N. Chen, J. Cheng, S.-M. Zhuang, L. Zheng, Blood, 110 (2007) 587-595.
[34] T. Kobayashi, T. Chanmee, N. Itano, Biomolecules, 10 (2020) 1525.
[35] S. Garantziotis, R.C. Savani, Matrix Biology, 78-79 (2019) 1-10.
[36] J.E. Rayahin, J.S. Buhrman, Y. Zhang, T.J. Koh, R.A. Gemeinhart, ACS Biomaterials Science & Engineering, 1 (2015) 481-493.
[37] B.M. Lee, S.J. Park, I. Noh, C.-H. Kim, Biomaterials Research, 25 (2021) 27.
[38] D.B. Lyle, J.C. Breger, L.F. Baeva, J.C. Shallcross, C.N. Durfor, N.S. Wang, J.J. Langone, Journal of Biomedical Materials Research Part A, 94A (2010) 893-904.
[39] L.F. Baeva, D.B. Lyle, M. Rios, J.J. Langone, M.M. Lightfoote, Journal of Biomedical Materials Research Part A, 102 (2014) 305-314.
[40] C.K. Hee, D.J. Messina, Journal of Immunology and Regenerative Medicine, 17 (2022) 100065.
[41] Y. Dong, A. Arif , M. Olsson, V. Cali, B. Hardman, M. Dosanjh, M. Lauer, R.J. Midura, V.C. Hascall, K.L. Brown, P. Johnson, Scientific Reports, 6 (2016) 36928.
[42] H. Kim, J. Cha, M. Jang, P. Kim, Biomaterials Science, 7 (2019) 2264-2271.
[43] D. Petta, A.R. Armiento, D. Grijpma, M. Alini, D. Eglin, M. D'Este, Biofabrication, 10 (2018) 044104.
[44] K.S. Kim, S.J. Park, J.A. Yang, J.H. Jeon, S.H. Bhang, B.S. Kim, S.K. Hahn, Acta Biomaterialia, 7 (2011) 666-674.
[45] C. Loebel, S.E. Szczesny, B.D. Cosgrove, M. Alini, M. Zenobi-Wong, R.L. Mauck, D. Eglin, Biomacromolecules, 18 (2017) 855-864.
[46] R. Wang, X. Huang, B. Zoetebier, P.J. Dijkstra, M. Karperien, Bioactive Materials, 20 (2023) 53-63.
[47] L.-S. Wang, F. Lee, J. Lim, C. Du, A.C.A. Wan, S.S. Lee, M. Kurisawa, Acta Biomaterialia, 10 (2014) 2539-2550.
[48] A. Schwab, C. Hélary, R.G. Richards, M. Alini, D. Eglin, M. D'Este, Materials Today Bio, 7 (2020) 100058.
[49] C. Loebel, M. D'Este, M. Alini, M. Zenobi-Wong, D. Eglin, Carbohydrate Polymers, 115 (2015) 325-333.
[50] S.H. Rhee, Intest Res, 12 (2014) 90-95.
[51] F. Razzi, L.E. Fratila-Apachitei, N. Fahy, Y.M. Bastiaansen-Jenniskens, I. Apachitei, E. Farrell, A.A. Zadpoor, Biomed Mater, 15 (2020) 035017.
[52] L. Utomo, G.S.A. Boersema, Y. Bayon, J.F. Lange, G. van Osch, Y.M. Bastiaansen-Jenniskens, Biomed Mater, 12 (2017) 025006.
[53] U.D.o.H.a.H. Services., F.a.D. Administration., C.f.D.E.a. Research., C.f.B.E.a. Research., C.f.V. Medicine., C.f.D.a.R. Health., O.o.R.A. (ORA). in: U.S.D.o.H.a.H. Services (Ed.), Food and Drug Administration, 2012.
[54] P. Pelegrin, A. Surprenant, The EMBO Journal, 28 (2009) 2114-2127.
[55] H.M. Rostam, P.M. Reynolds, M.R. Alexander, N. Gadegaard, A.M. Ghaemmaghami, Scientific Reports, 7 (2017) 3521.
[56] R. Sridharan, B. Cavanagh, A.R. Cameron, D.J. Kelly, F.J. O'Brien, Acta Biomaterialia, 89 (2019) 47-59.
[57] C. Mondadori, A. Chandrakar, S. Lopa, P. Wieringa, G. Talò, S. Perego, G. Lombardi, A. Colombini, M. Moretti, L. Moroni, Bioactive Materials, 21 (2023) 209-222.
[58] D.A. Chistiakov, M.C. Killingsworth, V.A. Myasoedova, A.N. Orekhov, Y.V. Bobryshev, Laboratory Investigation, 97 (2017) 4-13.
[59] J. Sapudom, S. Karaman, W.K.E. Mohamed, A. Garcia-Sabaté, B.C. Quartey, J.C.M. Teo, npj Regenerative Medicine, 6 (2021) 83.

[60] G.F. Vasse, P.T. Kühn, Q. Zhou, S.A. Bhusari, C. Reker-Smit, B.N. Melgert, P. van Rijn, Journal of Immunology and Regenerative Medicine, 1 (2018) 13-20.
[61] P. Italiani, D. Boraschi, Frontiers in immunology, 5 (2014) 514.
[62] N. Haddy, C. Sass, S. Maumus, B. Marie, S. Droesch, G. Siest, D. Lambert, S. Visvikis, European Journal of Human Genetics, 13 (2005) 109-117.
[63] K.L. Singampalli, S. Balaji, X. Wang, U.M. Parikh, A. Kaul, J. Gilley, R.K. Birla, P.L. Bollyky, S.G. Keswani, Front Cell Dev Biol, 8 (2020) 636.
[64] C. Hedrich, J. Bream, Immunologic research, 47 (2010) 185-206.
[65] L.K. Kozicky, S.C. Menzies, Z.Y. Zhao, T. Vira, K. Harnden, K. Safari, K.L. Del Bel, S.E. Turvey, L.M. Sly, Frontiers in Immunology, 9 (2018).
[66] P.B. Wright, E. McDonald, A. Bravo-Blas, H.M. Baer, A. Heawood, C.C. Bain, A.M. Mowat, S.L. Clay, E.V. Robertson, F. Morton, J.S. Nijjar, U.Z. Ijaz, S.W.F. Milling, D.R. Gaya, Scientific Reports, 11 (2021) 19616.
[67] B.O. Fabriek, C.D. Dijkstra, T.K. van den Berg, Immunobiology, 210 (2005) 153-160.
[68] S.D. Jayasingam, M. Citartan, T.H. Thang, A.A. Mat Zin, K.C. Ang, E.S. Ch'ng, Frontiers in Oncology, 9 (2020).
[69] I. Kwiecień, M. Polubiec-Kownacka, D. Dziedzic, D. Wołosz, P. Rzepecki, J. Domagała-Kulawik, Central European Journal of Immunology, 44 (2019) 395-402.